Variable superconducting quantum-interference device: Theory

H. J. Fink, V. Grünfeld,* and S. M. Roberts†
Department of Electrical and Computer Engineering, University of California, Davis, Davis, California 95616
(Received 1 October 1986)

A dc superconducting quantum interference device (SQUID) consisting of a symmetric ring circuit with four Josephson junctions and two independent external currents I_1 and I_2, which enter the circuit at different points, has a phase boundary between the fully superconducting and the normal states that is different from that of a conventional SQUID. The control current I_2 modifies the magnetic flux (ϕ) periodicity and the value of the maximum measuring current $I_{1m}(\phi)$. For values of $I_2 > I_c$ (critical current of Josephson junction) the fully resistive state exists over flux intervals centered around $(n+\frac{1}{2})\phi_0$, where n is an integer and ϕ_0 is the fluxoid quantum. A superconducting circuit without Josephson junctions is suggested which should have a phase boundary similar to that found here. Minimization procedures which are usually employed in analyzing SQUID's are discussed.

I. INTRODUCTION

Shortly after the discovery of the Josephson effect,[1,2] Jaklevic *et al.*[3,4] developed a dc superconducting quantum interference device (SQUID) consisting of two Josephson (tunnel) junctions in parallel in a ring circuit. This device has been used up to the present as the basic element for very sensitive measuring instruments. Possibly the earliest and most general analysis of double junctions has been that of Fulton, Dunkleberger, and Dynes[5] which requires graphical methods and is valid for any form of the current-phase relation. Later, using the method of Lagrange multipliers, Tsang and Van Duzer[6] found the maximum zero-voltage direct current of arrays, each loop of which contained two Josephson junctions (JJ's). Similarly, Schulz-DuBois and Wolf[7] calculated the static characteristics of interferometers starting with the Gibbs free energy. This procedure is analogous to that employed in Ref. 6 and leads to similar results. Here again, only two JJ's were contained in each loop. Peterson and Hamilton[8] extended the analysis of Ref. 6 and Peterson and McDonald[9] obtained the average voltage and circulating current of a two JJ dc SQUID. Recently, Blackburn[10] analyzed the stationary states and flux dynamics of rings containing N ($=5$) JJ's in an isolated ring circuit *without* any current injected from an external source. McDonald[11] simulates a SQUID which contains a loop with four JJ's (rather than the usual one or two) for the purpose of amplification by phase locking. It allows direct, instead of inductive, coupling to the SQUID and possibly an extended response to higher frequencies.

Logic gates have also been developed experimentally[12–14] which incorporate ring circuits with four JJ's but are operated as three terminal devices as in Ref. 11. Because of the potential applications of a four JJ's ring circuit in devices, we have found it worthwhile to investigate theoretically the detailed properties of a SQUID circuit consisting of four JJ's and operated as a four-terminal device controlled by two independent external current sources and an applied magnetic field perpendicular to the ring circuit. First the salient features of a conventional dc SQUID circuit will be summarized and used later for the derivation of the variable SQUID (VSQUID). We shall comment in the Appendix on the above minimization procedures which keep the applied flux constant.

II. SQUID THEORY

The salient features of a superconducting quantum interference device are shown schematically in Fig. 1(a). It consists of two JJ's, denoted by crosses, connected in parallel in a ring circuit which is constructed of superconducting wires. An external current I is supplied from an outside source to node A and extracted from node B. A magnetic field **B** is applied perpendicular to the ring which causes an internal magnetic flux ϕ to be locked-in within the ring circuit and which can be measured directly.[15] The flux difference between the internal and applied flux is proportional to a persistent current in the ring. For a fixed value of the enclosed magnetic flux ϕ there exists a maximum value of the current I, I_m, at which a

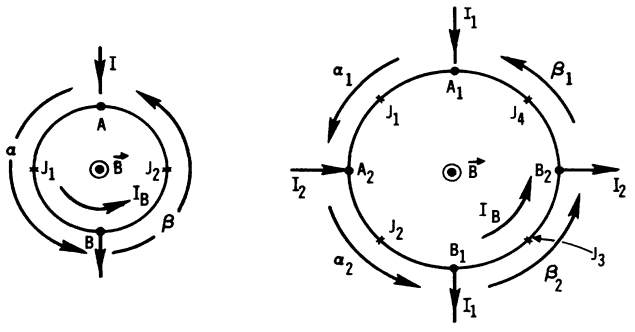

FIG. 1. Schematic diagram of (a) conventional SQUID circuit with two Josephson junctions and one external current source, and (b) variable SQUID (VSQUID) circuit with four Josephson junctions and two independent external current supplies. For details see text.

finite electric potential difference, V, between nodes A and B is established. For $I < I_m(\phi)$ the value of $V=0$. We shall denote the dephasing angle from A to B along J_1 as α and that from B to A along J_2 as β. For a practical device which incorporates tunnel junctions, α and β lie almost entirely across J_1 and J_2, respectively. For simplicity we assume that the magnetic flux inside the JJ's can be ignored, that the loop is symmetric, that all JJ's are identical, that each JJ has a critical current I_c and that volume effects of the wires are negligible.

The fluxoid relation, obtained from a contour integration of the second Ginzburg-Landau (GL) equation, is

$$n\phi_0=\phi+\frac{\phi_0}{2\pi}\oint\frac{\mathbf{J}\cdot d\mathbf{x}}{f^2}\ , \tag{1}$$

where n is a positive or negative integer or zero, ϕ_0 the fluxoid quantum ($=h/2e$), $f(x)$ the modulus of the normalized GL order parameter, J the GL normalized current density, and x the curvilinear coordinate along the contour which encloses the total magnetic flux ϕ. The value of $\mathbf{x}$ is normalized by the GL coherence length $\xi(t)$. The applied flux ϕ_a is then related to ϕ by

$$\phi=\phi_a+LI_B \tag{2}$$

where L, the self-inductance of the loop, ϕ, ϕ_a, and I_B are in mks units.

With the definitions

$$i=I/2I_c\ ,$$

$$i_b=I_B/I_c\ ,$$

the Josephson relations across J_1 and J_2 are

$$i_b+i=\sin\alpha\ , \tag{3}$$

$$i_b-i=\sin\beta\ . \tag{4}$$

It should be recognized that the ratio J/f^2 in Eq. (1) is the superfluid velocity $\mathbf{Q}=\xi(\nabla\varphi-2\pi\mathbf{A}/\phi_0)$, where $\varphi(x)$ is the phase of the order parameter and $\mathbf{A}$ is the vector potential. It then follows that the line integral of J/f^2 from A to B via J_1 for the SQUID in Fig. 1(a) is the gauge-invariant dephasing angle α which is not the same as $\Delta\varphi$, the change in the phase of the order parameter between A and B via J_1.

For single-valuedness of the order parameter, the sum of all the $\Delta\varphi$'s around a closed path must be $2\pi n$, but the sum of the dephasing angles around a closed path is not equal to $2\pi n$ unless the enclosed flux is zero. This follows from Eq. (1'') and this concept has been explained clearly by Deaver[16] and Webb.[17] There has been, however, some confusion with its interpretation in the literature (cf. Ref. 7 where the phase change $\Delta\varphi$ is assumed to drive the JJ's). We thus identify the integral on the right-hand side of Eq. (1) with $\alpha+\beta$ so that Eq. (1) with the definition

$$\chi=\frac{\pi}{2}[n-(\phi/\phi_0)] \tag{1'}$$

becomes

$$4\chi=\alpha+\beta\ . \tag{1''}$$

Defining the phase difference across the SQUID (between nodes A and B) by

$$2\delta=\alpha-\beta\ ,$$

Eqs. (3) and (4) can also be written as

$$i_b=\sin(2\chi)\cos\delta \tag{5}$$

$$i=\cos(2\chi)\sin\delta\ . \tag{6}$$

It is apparent from Eq. (6) that the maximum value of i, i_m, is reached when $\delta=\pi/2$ at which value $i_b=0$. We shall comment on finding the extremum of i in the Appendix. It also follows from Eqs. (5) and (6) that

$$i_b=\tan(2\chi)(\cos^2 2\chi-i^2)^{1/2}\ . \tag{7}$$

The reason why a device such as that shown in Fig. 1(a) is called an interferometer is that the phase boundary between the resistive and zero resistance state is periodic in ϕ/ϕ_0, similar to that of a Fraunhofer interference pattern in optics.

The natural variable in Eqs. (5) and (6) is χ, which is proportional to the total enclosed flux in the ring or, in other words, the magnetic flux which is locked-in in the ring circuit. The latter can be measured directly[15] (at least the corresponding value of the enclosed magnetic flux density). It is then advantageous, simpler and more general to use χ as a variable in finding the maximum supercurrent, i_m, instead of the applied flux ϕ_a. This result is valid for any nonlinear inductance L. Once i_m and the corresponding value of i_b are known, the applied flux ϕ_a can be calculated from Eq. (2) provided the value of the nonlinear inductance L at that particular value of i_b is given (see Appendix).

III. VSQUID

It will be shown that one can control the shape of the phase boundary between the zero resistance and the resistive state by a modification of the SQUID circuit shown schematically by the circuit of Fig. 1(b). Comparing Figs. 1(a) with 1(b), we replace the current I by I_1, the junction J_1 by the junctions J_1 and J_2, and the junction J_2 by the junctions J_3 and J_4. An additional control current I_2 is introduced as shown in Fig. 1(b). The external currents I_1 and I_2 are controlled by independent sources. A voltage appears between nodes A_1 and B_1 when, for a constant value of the control current, I_2, the measuring current, I_1, exceeds a maximum value, a behavior similar to that of a conventional SQUID. As in Fig. 1(a), a flux ϕ links the loop, giving rise to the circulating persistent current I_B when $\phi\neq\phi_a$. Defining

$$i_1=I_1/2I_c\ ,$$

$$i_2=I_2/2I_c\ ,$$

$$i_b=I_b/I_c\ ,$$

the appropriate Josephson relations are

$$i_1-i_2+i_b=\sin\alpha_1\ , \tag{8}$$

$$i_1+i_2+i_b=\sin\alpha_2\ , \tag{9}$$

$$-i_1-i_2+i_b=\sin\beta_1 \ , \tag{10}$$

$$-i_1+i_2+i_b=\sin\beta_2 \ , \tag{11}$$

where α_1, α_2, β_2, and β_1 are the dephasing angles across the junctions J_1 to J_4. Solving Eqs. (8)–(11) for i_1, i_2, and i_b in terms of the α's and β's, one finds that the following relation must be satisfied:

$$\sin\alpha_2-\sin\alpha_1=\sin\beta_2-\sin\beta_1 \ . \tag{12}$$

With the same definition of χ as above, Eq. (1), analogous to Eq. (1''), becomes

$$4\chi=\alpha_1+\alpha_2+\beta_2+\beta_1 \ . \tag{13}$$

Defining the phase difference between A_1 and B_1, $4\delta_1$, and between A_2 and B_2, $4\delta_2$, by

$$4\delta_1=(\alpha_1+\alpha_2)-(\beta_1+\beta_2) \ , \tag{14}$$

$$4\delta_2=(\alpha_2+\beta_2)-(\alpha_1+\beta_1) \ , \tag{15}$$

and using Eqs. (12) and (13), the solutions for the currents, after some lengthy manipulations, take on the form

$$i_1=(1/2D)\cos(\chi+\delta_2)\cos(\chi-\delta_2)\sin(2\delta_1) \ , \tag{16}$$

$$i_2=(1/2D)\cos(\chi+\delta_1)\cos(\chi-\delta_1)\sin(2\delta_2) \ , \tag{17}$$

$$i_b=(1/2D)\cos(\delta_1+\delta_2)\cos(\delta_1-\delta_2)\sin(2\chi) \ , \tag{18}$$

with D being

$$D=\pm[\cos^2\delta_1\cos^2\delta_2 -\sin^2\chi\cos(\delta_1+\delta_2)\cos(\delta_1-\delta_2)]^{1/2} \ . \tag{19}$$

Equation (16) can be cast also into the following form which will be useful when discussing Fig. 2:

$$i_1=\cos\chi\sin\delta_1\frac{1-\left[\dfrac{\sin\delta_2}{\cos\chi}\right]^2}{\left\{1-\left[\dfrac{\sin\delta_2}{\cos\chi}\right]^2\left[1-\left[\dfrac{\sin\chi}{\cos\delta_1}\right]^2\right]\right\}^{1/2}} \ . \tag{16'}$$

When the control current $i_2=0$, Eqs. (16') and (18) become

$$i_1=\cos\chi\sin\delta_1 \ , \tag{20}$$

$$i_b=\sin\chi\cos\delta_1=\tan\chi(\cos^2\chi-i_1^2)^{1/2} \ . \tag{21}$$

Finding solutions of the implicit Eqs. (16)–(18) for the VSQUID and its resistive phase boundary is by no means as simple as solving Eqs. (5) and (6) for the conventional SQUID. Although it is, in principle, possible to minimize the Gibbs free energy[7] or to use Lagrange multipliers,[6] we found it in our case considerably simpler to obtain a numerical solution by reasoning as follows: I_1, I_2, and ϕ_a are controlled by independent external sources, and ϕ_a is related to ϕ and I_B through Eq. (2) provided L is known. We thus choose i_1, i_2, and χ [Eq. (1')] to be the primary variables in Eqs. (16)–(18) and δ_1, δ_2, and i_b the secondary.

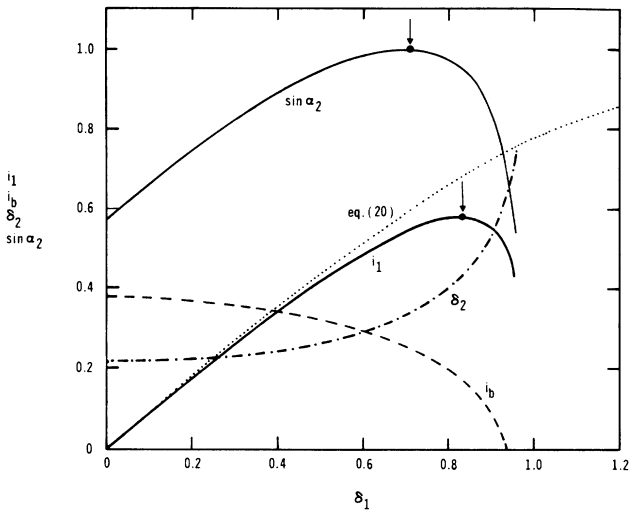

FIG. 2. Solutions of Eqs. (16)–(19) for the VSQUID with $i_2=0.2$ and $\chi=0.4$ which are compared with Eq. (20) ($i_2=0$, dotted curve). The maximum of $\sin\alpha_2=i_1+i_2+i_b$ [Eq. (9)] occurs at $\delta_1=0.707$ while the maximum of i_1 ($=i_{1m}$) is reached at $\delta_1=0.827$. i_1 is the measuring and i_2 the control current of the VSQUID, i_b the circulating current in the ring, and $4\delta_1$ and $4\delta_2$ are the phase differences of the dephasing angles [Eqs. (14) and (15)] between the nodes A_1 and B_1, and A_2 and B_2 of Fig. 1(b). For $i_1>i_{1m}$ a voltage appears between A_1 and B_1 while for $i_1<i_{1m}$ the voltage is zero.

We assume that i_1 as a function of δ_1 and its maximum value, i_{1m}, can be found by keeping the control current i_2 and the total enclosed flux χ in the ring circuit constant. It is then possible to solve Eq. (17) for $\sin\delta_2$ in terms of δ_1, χ, and i_2. Then $\sin\delta_2$ is substituted into Eq. (16) and i_1 is found as a function of δ_1 up to its maximum value for constant values of χ and i_2. Simultaneously Eqs. (8)–(11) are satisfied. The corresponding value of i_b is obtained from Eq. (18).

Figure 2 shows a typical plot of i_1, i_b, $\sin\alpha_2$, and δ_2 as a function of δ_1 for $i_2=0.2$ and $\chi=0.4$. As δ_1 increases, $\sin\alpha_2=i_1+i_2+i_b$ reaches a maximum before the measuring current i_1 reaches its maximum value. This is due to the rapid decrease of i_b for large values of δ_1. The value of δ_1 for which $\sin\alpha_2=1$ can be obtained from $\delta_1=\cos^{-1}(i_2)^{1/2}-\chi$. The maximum of i_1 occurs always at a value of δ_1 which is larger than the δ_1 value corresponding to the maximum of $i_1+i_2+i_b$, except when $\chi=0$ or $i_{1m}\to 0$, in which cases the maxima occur at the same value of δ_1. When i_1 is increased by the external source beyond its maximum value, i_{1m}, a finite voltage appears between the nodes A_1 and B_1 and the solutions to the right of i_{1m} are of no physical significance. However, the solutions to the right of the maximum value of $\sin\alpha_2$, up to the maximum of i_1, are physically correct solutions in spite of the fact that the total current through junction J_2 has reached its critical current I_c at a smaller I_1 value. The dotted curve is i_1 for $i_2=0$, Eq. (20), which reaches

its maximum value at $\delta_1=\pi/2$. As can be seen from the numerator of Eq. (16′) and Fig. 2, the rapid increase in δ_2 is linked to the fact that when $i_2\neq 0$ the function i_1 reaches a maximum before $\delta_1=\pi/2$. In fact, a very small control current i_2 has a very large effect on destroying the symmetry of the circuit and changes drastically the phase boundary between the superconducting and finite resistance states of the VSQUID. This is shown in Fig. 3. The results of Fig. 2 are correct, in general, when any of the signs of i_2, δ_1, and χ are reversed since the circuit shown in Fig. 1(b) is invariant under permutations of the four junctions or a relabeling of the four branches. The measuring current i_1 is an odd function of δ_1.

By finding i_{1m} for various constant values of i_2 and χ we obtained i_{1m} as a function of ϕ/ϕ_0 for various constant control currents i_2. Figure 3 shows the results for $i_2=0$, 0.01, 0.2, 0.5, and 0.8 and Fig. 4 the corresponding values of i_b at i_{1m} as a function of ϕ/ϕ_0-n. From the data of Fig. 4 the values of ϕ_a can be obtained at the resistive phase boundary provided L is known [Eq. (2)]. For comparison, the conventional SQUID, Eq. (6), with $\delta=\pi/2$, is shown in Fig. 3 by the dashed curve. The corresponding i_b value is zero for the conventional SQUID [Eq. (5) with $\delta=\pi/2$].

The results of Fig. 3 show that the resistive phase boundary of the VSQUID is strongly modified by the control current i_2 and that for $i_2=0$ the phase boundary of a VSQUID is different from that of a conventional SQUID. It is apparent that for $i_2=0$ the VSQUID has, for the same quantum number n, a larger zero-voltage dc current $|i_{1m}|$, than the conventional SQUID, $|i_m|$.

The reader should note that the abscissae in Figs. 3 and

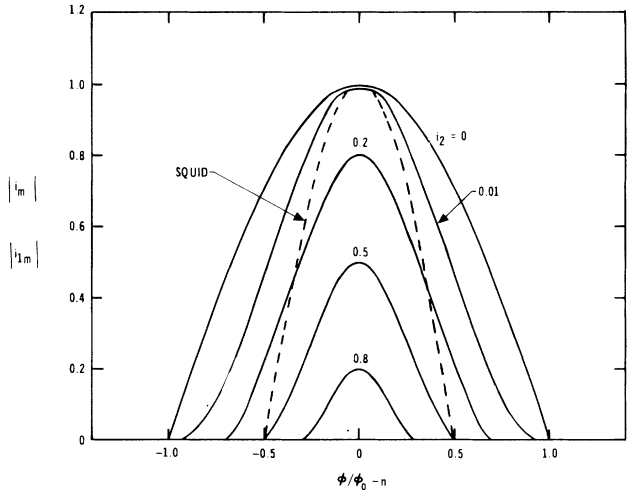

FIG. 3. Shown is the phase boundary ($|i_{1m}|$) between the zero resistance (region below the curve) and finite resistance states (region above curve) for a VSQUID for various control currents i_2 as a function of (ϕ/ϕ_0-n), where ϕ is the total flux. The values of n are quantum numbers and ϕ_0 is the fluxoid quantum. The dashed curve is the phase boundary ($|i_m|$) of a conventional SQUID [Eq. (6) with $\delta=\pi/2$]. Note that $|i_{1m}|>|i_m|$ for the same value of n. Volume effects of the superconducting wires and junctions have been neglected. All curves are periodic in ϕ/ϕ_0.

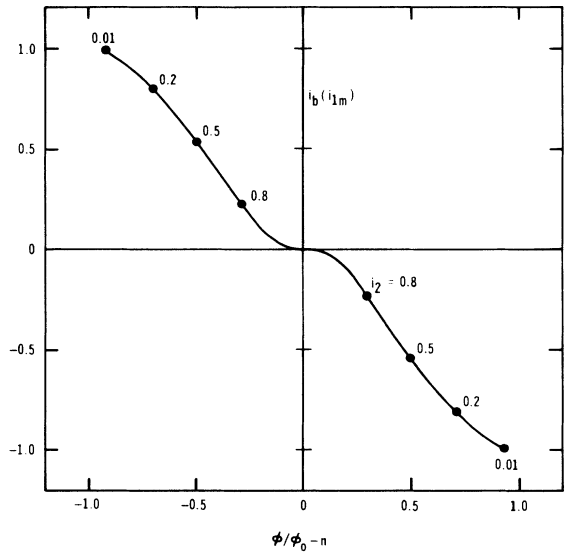

FIG. 4. Shown is the circulating current i_b of the VSQUID at the maximum supercurrent $|i_{1m}|$ (same as that shown in Fig. 3) as a function of (ϕ/ϕ_0-n) for various control currents i_2 (>0) and various quantum numbers n. The dots mark the maximum value of (ϕ/ϕ_0-n) up to which i_b can increase for a fixed i_2. For the conventional SQUID $i_b=0$ at $|i_m|$. For details see text.

4 are ϕ/ϕ_0-n. Therefore, the results of $|i_{1m}|$ and i_b are periodic in ϕ/ϕ_0. In Fig. 4 we have marked with dots the maximum value of (ϕ/ϕ_0-n) up to which i_b can increase for a fixed value of i_2 (also indicated on the graph). Although it might seem that the values of i_b at i_{1m} lie on a universal curve for the various i_2 values, in fact this is so only within the graphical accuracy.

From Fig. 3 it becomes apparent, because of the periodicity, that for $i_2=0$ and $\phi/\phi_0=1$ the VSQUID can change from a quantum state with $n=0$ to one with either $n=1$ or 2, while for i_2 between zero and 0.5 the transition must occur from $n=0$ to $n=1$ only. For values of i_2 between 0.5 and 1.0 the superconducting state of the VSQUID is completely quenched for values of the flux in the neighborhood of $(n+1/2)\phi_0$, and for $i_2=1$ the VSQUID is always in the resistive state. For a conventional SQUID the quantum number at $|i_m|$ changes by an integer when $\phi=(n+1/2)\phi_0$, while for a VSQUID with $i_2=0$ and $n=0$, for example, this could be anywhere between $\phi=\phi_0/2$ and ϕ_0. If $i_2=0.5$, then the change of n occurs at $(n+\frac{1}{2})\phi_0$. For $i_2>0.5$ the circuit changes first from a superconducting state with quantum number n to the full resistive state when ϕ is changed, before a new quantum number $n\pm 1$ of the following superconducting state is attained. Thus the control current i_2 influences profoundly the superconducting-normal phase boundary and the possible quantum state the VSQUID assumes.

IV. CONCLUSIONS

A generalized superconducting quantum interference device with four Josephson junctions and with two in-

dependent external currents I_1 and I_2 [Fig. 1(b)] has a phase boundary between the zero resistance and a finite resistance state which is different from that of a conventional SQUID. The control current I_2 modifies the periodicity of the magnetic flux in terms of the magnetic fluxoid quantum, and the magnitude of the maximum supercurrent I_{1m} in terms of the critical current I_c of the Josephson junctions. For the larger control currents ($I_2 > I_c$) the device alternates between the superconducting state and the normal state as the applied magnetic field is changed. Thus a VSQUID turns out to be a device which has a flexible superconducting-normal phase boundary controlled by I_2.

The maximization of the measuring current I_1 was done numerically by keeping the control current I_2 and the enclosed flux constant and varying the phase difference across the VSQUID. Since the enclosed flux is the scalar sum of the applied and current generated fluxes, this is valid for any value of the latter. For our four JJ's VSQUID our numerical procedure was found to be simpler than the formal manipulations using Lagrange multipliers or the Gibbs free energy. Our maximization procedure is fairly simple and straightforward and allows for easy conversion between the possible states of independent variables, while keeping the inductance L as a phenomenologically defined quantity. No linearization approximations are made in our approach.

It is suggested that a ring circuit of radius of about one-half the coherence length, $\xi(t)$, with two independent external current sources should operate without Josephson junctions just like the above VSQUID. This is conjectured from the finding that a ring circuit without[18] Josephson junctions, of the appropriate size, with one independent external current source, performs like a conventional dc SQUID.

ACKNOWLEDGMENTS

This work was supported in part by the National Science Foundation under Grants Nos. ECS-8505627 and INT-8502375. We thank A. López for discussions.

APPENDIX

The method of constrained maximization as used, for example, in Refs. 6 and 7 applied to an ordinary two-junction SQUID circuit, involves finding the extrema of a function such as [cf. Ref. 6, Eq. (6)]

$$I_a(\phi_1,\phi_2,\lambda)=i_{c1}\sin\phi_1+i_{c2}\sin\phi_2 + \lambda(\phi_1-\phi_2+\theta_a+\alpha_1\sin\phi_1-\alpha_2\sin\phi_2)$$

with

$$\alpha_1=\frac{2\pi}{\phi_0}L_1 i_{c1},\quad \alpha_2=\frac{2\pi}{\phi_0}L_2 i_{c2},\quad \theta_a=\frac{2\pi}{\phi_0}\phi_a\ .$$

Here ϕ_a is the applied magnetic flux, (L_1+L_2) is the inductance of the loop and λ is the Lagrange indetermined multiplier. A deeper analysis[16] shows that L_1 and L_2 depend on the currents in the branches, thus on ϕ_1 and ϕ_2. If the nonlinear character of the inductance were to be taken into account, using the Lagrange method, the ensuing equations would become extremely clumsy and difficult to handle even for the case of the two junction SQUID. In our approach this is avoided, and exact solutions are found for the combined Josephson and Ginzburg-Landau relations, together with fluxoid quantization. We thus think our method is more convenient and useful.

*Permanent address: Centro Atómico Bariloche, 8400-Bariloche, Argentina.

†Present address: Revelle College, University of California, San Diego, CA 92093.

[1]B. D. Josephson, Phys. Lett. **1**, 251 (1962).

[2]P. W. Anderson and J. M. Rowell, Phys. Rev. Lett. **10**, 230 (1963).

[3]R. C. Jaklevic, J. Lambe, A. H. Silver, and J. E. Mercerau, Phys. Rev. Lett. **12**, 159 (1964).

[4]P. C. Jaklevic, J. Lambe, J. E. Mercerau, and A. H. Silver, Phys. Rev. **140A**, 1628 (1965).

[5]T. A. Fulton, D. L. Dunkleberger, and R. C. Dynes, Phys. Rev. B **6**, 855 (1972).

[6]W.-T. Tsang and T. Van Duzer, J. Appl. Phys. **46**, 4573 (1975).

[7]E. O. Schulz-Dubois and P. Wolf, Appl. Phys. **16**, 317 (1978).

[8]R. L. Peterson and C. A. Hamilton, J. Appl. Phys. **50**, 8135 (1979).

[9]R. L. Peterson and D. G. McDonald, J. Appl. Phys. **54**, 992 (1983).

[10]J. A. Blackburn, J. Appl. Phys. **56**, 1477 (1984).

[11]D. G. McDonald, Appl. Phys. Lett. **45**, 1243 (1984).

[12]H. Nakagawa, E. Sogawa, S. Kosaka, S. Takada, and H. Hayakawa, Jpn. J. Appl. Phys. **21**, L198 (1982).

[13]T. Kobayashi, K. Hamasaki, N. Kondoh, T. Komata, and T. Yamashita, Appl. Phys. Lett. **42**, 475 (1983).

[14]E. Sogawa, H. Nakagawa, S. Takada, and H. Hyakawa, Jpn. J. Appl. Phys. **22**, L642 (1983).

[15]W. L. Goodman, W. D. Willis, D. A. Vincent, and B. S. Deaver, Jr., Phys. Rev. B **4**, 1530 (1971).

[16]B. S. Deaver, Jr., *The Science and Technology of Superconductivity*, edited by W. D. Gregory and W. N. Matthews, Jr. (Plenum, New York, 1973), pp. 539.

[17]W. W. Webb, *The Science and Technology of Superconductivity*, Ref. 16, p. 653.

[18]H. J. Fink, V. Grünfeld, and A. López, Phys. Rev. B **35**, 35 (1987).